Nuclear Engineering and Technology 51 (2019) 337–344

Contents lists available at ScienceDirect

Nuclear Engineering and Technology

journal homepage: www.elsevier.com/locate/net

Original Article

Computational design and characterization of a subcritical reactor assembly with TRIGA fuel

Alvie Asuncion-Astronomo [a, *], Žiga Štancar [b], Tanja Goričanec [b], Luka Snoj [b]

[a] Philippine Nuclear Research Institute, Diliman, Quezon City, 1101, Philippines
[b] Jožef Stefan Institute, Jamova cesta 39, SI-1000, Ljubljana, Slovenia

ARTICLE INFO

Article history:
Received 9 July 2018
Received in revised form
18 September 2018
Accepted 29 September 2018
Available online 1 October 2018

Keywords:
Nuclear reactor
Subcritical assembly
TRIGA fuel
MCNP

ABSTRACT

The TRIGA fuel of the Philippine Research Reactor-1 (PRR-1) will be used in a subcritical reactor assembly (SRA) to strengthen and advance nuclear science and engineering expertise in the Philippines. SRA offers a versatile and safe training and research facility since it can produce neutrons through nuclear fission reaction without achieving criticality. In this work, we used a geometrically detailed model of the PRR-1 TRIGA fuel to design a subcritical reactor assembly and calculate physical parameters of different fuel configurations. Based on extensive neutron transport simulations an SRA configuration is proposed, comprising 44 TRIGA fuel rods arranged in a 7 × 7 square lattice. This configuration is found to have a maximum k_{eff} value of 0.95001±0.00009 at 4 cm pitch. The SRA is characterized by calculating the 3-dimensional neutron flux distribution and neutron spectrum. The effective delayed neutron fraction and mean neutron generation time of the system are calculated to be 748 pcm±7 pcm and 41 μs, respectively. Results obtained from this work will be the basis of the core design for the subcritical reactor facility that will be established in the Philippines.

1. Introduction

The Philippine Nuclear Research Institute (PNRI) used to operate the Philippine Research Reactor-1 (PRR-1), which is the only nuclear facility that was utilized in the Philippines. The facility was the focal point of nuclear expertise in the country during its operation from 1963 to 1984. In 1984, PRR-1 was upgraded into a 3 MW TRIGA reactor but it was rendered inoperable in 1988 due to an unresolved technical problem. The TRIGA fuel rods, which were provided as part of the PRR-1 upgrade, were only slightly irradiated during the conversion testing. These fuel rods have remained unused for 30 years since 1988. The absence of an operating nuclear facility resulted in the decline of expertise in nuclear science and engineering in the country. To augment this problem, PNRI decided in 2014 to re-operate PRR-1 using the slightly irradiated TRIGA fuel in a subcritical reactor assembly (SRA). This planned facility will be utilized for training, education and basic research to rebuild the country's human capacity in nuclear science and engineering. The planned SRA will be contained in the existing reactor pool inside the PRR-1 building as illustrated in Fig. 1.

A subcritical reactor is a nuclear fission reactor with a neutron multiplication factor $k_{eff} < 1$, which means that the system requires an external neutron source to sustain fission chain reaction. Isotopic neutron sources such as ^{239}Pu-Be, ^{252}Cf, ^{226}Ra-Be are typically used to drive SRAs [1–3]. Accelerators that produce neutrons via spallation reaction are also used as a neutron source for accelerator driven systems (ADS) where a particle accelerator is coupled to a nuclear reactor [4–7]. SRAs are used for research, education and training in the field of nuclear science and engineering around the world. Source driven sources are utilized to measure neutron noise and reactor kinetic parameters, as well as to validate neutron flux and reactor power calculations [2] [3], [8]. Accelerator driven subcritical systems, which operate with high energy neutrons, are also known to have very good potential for nuclear waste transmutation [6], [9–11]. Compared to critical reactor systems ($k_{eff} = 1$), SRAs offer a facility for training and basic research, which is relatively safer due to lesser radiation exposure and lower risk of criticality accident [6], [12]. This makes it an ideal starting nuclear facility for Philippines which is resuming a nuclear science and technology program. The plan is to build a critical mass of manpower knowledgeable on nuclear science through the operation of the PRR-1 SRA while investigating the feasibility of proceeding to a critical assembly.

* Corresponding author.
E-mail address: ajasuncion@pnri.dost.gov.ph (A. Asuncion-Astronomo).

https://doi.org/10.1016/j.net.2018.09.025

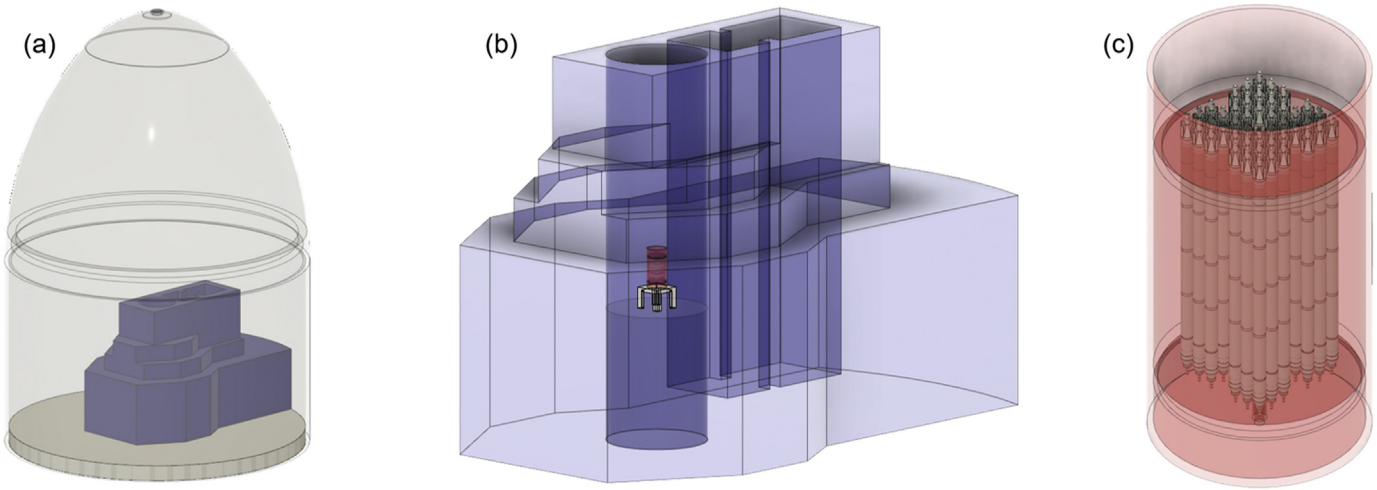

Fig. 1. Layout designs of PRR-1 (a) dome-shaped building with the reactor pool; (b) reactor pool with the proposed location of the SRA; and (c) the proposed fuel assembly in the core tank.

The aim of this work is to design an optimal subcritical core configuration for the PRR-1 TRIGA fuel rods and thoroughly analyze its neutronic characteristics, together with the supporting structures and proposed irradiation facilities. We employed a detailed model of the PRR-1 TRIGA fuel rod based on actual design parameters to simulate different core configurations using MCNP5 v.1.6 transport code [13]. Since the PRR-1 originally featured a rectangular lattice, it was decided to keep such lattice also for the SRA.

The fuel configuration chosen, with $k_{eff} = 0.95001$, contains 44 fuel rods arranged in a 7 × 7 square lattice at 4 cm pitch. The neutron flux profile, the effective delayed neutron fraction (β_{eff}), and mean neutron generation time (Λ) of the system are also presented in this paper.

2. Reactor physics of subcritical systems

Since subcritical reactors are operated with an external neutron source (NS), it is expected that its neutron flux profile will differ from the typical neutron distribution in a critical reactor. An external NS affects the reactor parameters of an SRA in at least two ways. First, the neutron multiplication factor of the SRA is influenced by two kinds of neutrons: neutrons born from fission events and neutrons from the NS. Second, the NS increases the flux level and distorts the neutron flux shape in the SRA [14] [15], which indicates that the power level of an SRA is dependent on the NS strength [16].

In order to account for these effects, deterministic calculation methods require a modification of static and dynamic point equations. Applicable equations have been derived for subcritical systems, which introduced a source multiplication factor k_s, in addition to the fission multiplication factor k_f [14] [17], [18]. The latter factor corresponds to the conventional k_{eff}. The contribution of each factor to the neutron multiplication factor of a subcritical system k_{sc} is expressed as [18]:

$$k_{sc} = \frac{k_f F + k_s S}{F + S} , \tag{1}$$

where F is the total number of fission neutrons and S is the total number of neutrons from the source. Another parameter that relates k_{sc} to k_{eff} is the neutron source efficiency. This parameter provides the relative importance of the source neutrons compared to fission neutrons and tends to be higher when the external source is placed in a high neutron-importance region [4] [19], [20].

Gandini [17] emphasized that the use of k_{sc} is pertinent for calculations of transients with broad time steps or for survey calculations well below criticality conditions. However, the use of the standard k_{eff} is recommended for analysis of accidental events in which the criticality condition may be surpassed during the transient [17]. As to the magnitude of difference between the factors, Nishihara's analytic solution for the stationary state shows that k_f and k_{eff} differed by 0.51% in a system with $k_{eff} = 0.95$, which is the target value for our system, and the two factors further agree for systems approaching criticality [18].

To determine the dependence of the subcritical neutron spectrum Φ on the external NS spectrum, the inhomogenous neutron balance equation in infinite medium is written as follows [14]:

$$\mathbf{A}\cdot\Phi = FX_f + SX_s , \tag{2}$$

where **A** is the removal operator which accounts for absorption and scattering of neutrons while X_i is the neutron emission spectrum vector for the fission source ($i = f$) and the external NS ($i = s$). In this treatment, neutron leakage is not accounted for and the infinite multiplication factors $k_{\infty f}$ and k_∞ are used instead of k_f and k_{eff}, respectively. The solution to Eq. (2) has been shown to have the following form [14]:

$$\Phi = S\left(\phi_s + \frac{\phi_c}{1/k_{\infty f} - 1}\right)k_\infty , \tag{3}$$

which suggests that for a deeply subcritical system ($k_{\infty f} \ll 1$), Φ tends to be closer to the shape of ϕ_s, which corresponds to the neutron spectrum of the external NS in a system with almost no fuel material. On the other hand, ϕ_c, which is the neutron spectrum of a critical reactor dominates over ϕ_s as the system approaches criticality ($k_{\infty f} \to 1$).

Deterministic codes, which rely on directly (commonly numerical) solving the neutron transport equation or diffusion equation to determine reactor parameters, require explicit formalisms to describe the behavior of subcritical reactor systems. On the other hand, Monte Carlo (MC) codes have the capability to calculate reactor parameters based on statistical averages of neutron

behavior by simulating a large number of neutron histories. Compared to deterministic codes, MC codes have the advantage of arbitrary geometry modelling and detailed representation of physical data since it does not require approximations. Although the two methods have fundamentally different approaches in calculating reactor parameters, they are expected to provide similar results when describing relatively simple systems. In this work the MCNP5 v.1.6 [13] MC particle transport code was used to calculate reactor parameters. MCNP is a well validated Monte Carlo radiation transport code that is capable of simulating neutron transport in complex three-dimensional systems.

3. Methods

3.1. Modeling of PRR-1 TRIGA fuel rods

The PRR-1 TRIGA fuel rod is 75.2 cm long and comprises 4 fuel elements (FE) composed of a solid homogenous mixture of U, Er, and a ZrH moderator. Each FE contains ~20 wt % uranium with 19.7% ^{235}U enrichment. The average uranium mass in each fuel rod is 427 $g \pm 3$ g. Erbium, a burnable poison mixed uniformly with the U–ZrH, accounts for 0.45 wt % of the fuel moderator while the H/Zr atom ratio is about 1.6. As shown in Fig. 2, the active section of the fuel-moderator rod has a diameter of 2.97 cm and is 50.8 cm long. The 4 FEs, the central Zr rod, the top and bottom graphite reflectors are enclosed in a 0.05 cm thick Incoloy-800 cladding with welded top and bottom fittings made of Inconel-600. For the calculations, we used a detailed fuel model based on these design parameters to simulate different TRIGA fuel rod configurations.

PRR-1 has a total of 130 TRIGA fuel rods, 115 of which were slightly irradiated when the PRR-1 conversion to TRIGA was tested in 1988, while 15 rods are completely fresh. Investigations on the effect of fuel burnup at the Istanbul Technical University (ITU) TRIGA reactor showed that a total burnup of 5.8 MWd resulted in only 1% reduction in the average thermal neutron flux in the core [21]. A study conducted at the Jožef Stefan Institute (JSI) TRIGA reactor reported that by accounting for the 2.2 MWd total burnup of their fuel rods, the k_{eff} of their reactor MC model decreased by 1.3% $\Delta k/k$ [22]. In comparison, the barely irradiated fuel rods of PRR-1 have a total core burnup of only 0.625 MWd, which is further divided among the 115 fuel rods. This warrants the use of fresh fuel parameters in our computational model.

The aim is to obtain a water moderated core configuration that utilizes the highest number of fuel rods but will remain subcritical. The acceptable range for the subcriticality margin is 5000 pcm±10% . To determine the desired core configuration, fuel rod models arranged in different configurations in square lattices were analyzed. The square lattice was chosen due to its symmetry and simple geometry implementation. The largest array analyzed in the simulation consists of 121 fuel rods in an 11 × 11 lattice, while the smallest consists of 36 rods in a 6 × 6 lattice. The fuel rod pitch for each array was varied from 3.5 cm to 6 cm at 0.5 cm interval to obtain the k_{eff} vs pitch plot for each lattice. Fig. 3 presents a sample MCNP model for the 11 × 11 lattice at 5 cm pitch, where the cylindrical aluminum core tank holding the fuel rods in place is shown. The aluminum tank is 101.5 cm long, 1.5 cm thick and has an inner diameter of 81 cm. The bottom and upper support plates are 2.5 cm and 2 cm thick, respectively. A water cylinder boundary that encloses the core tank with the fuel rod array, as shown in Fig. 3 (c), was also added to the model. The water boundary is 415 cm long and has a diameter of 261.6 cm, which corresponds to the actual diameter of the PRR-1 reactor pool.

3.2. Criticality calculations

The effective neutron multiplication factor k_{eff} of each fuel configuration was determined by performing criticality calculations (KCODE mode in MCNP) with MCNP5v.1.6 [13] and ENDF/B-VII.0 nuclear data library [23]. MCNP calculates k_{eff} by running successive fission cycles, which correspond to actual fission generations. Neutrons are terminated in each cycle, implying that the initial declaration of fission points only affects the first cycle. The effective

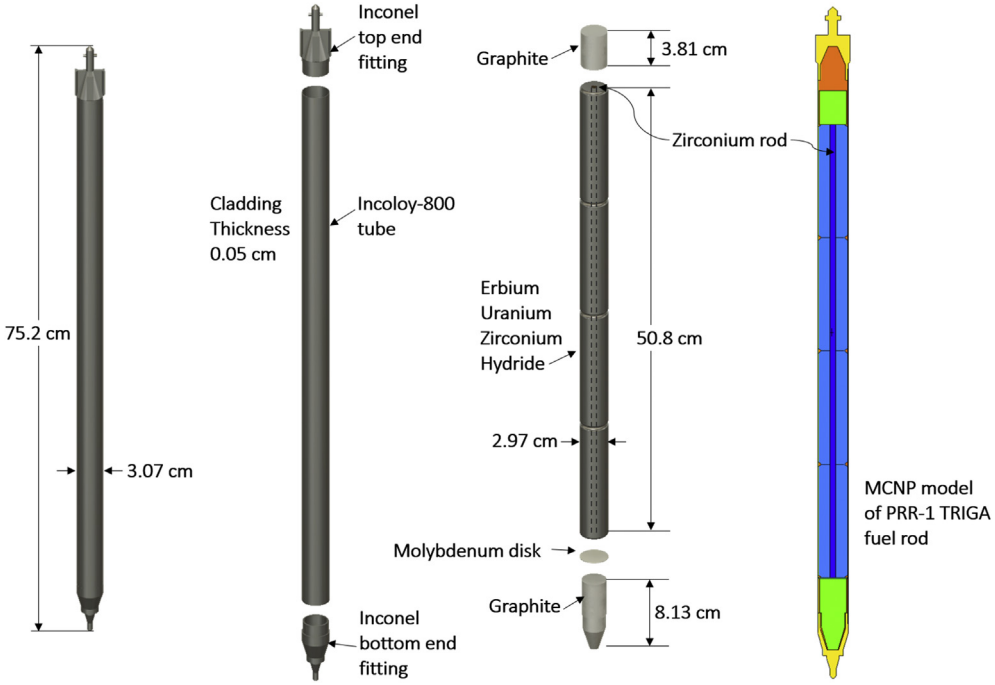

Fig. 2. PRR-1 TRIGA Incoloy-800 clad fuel-moderator and the vertical cross-section of its MCNP model.

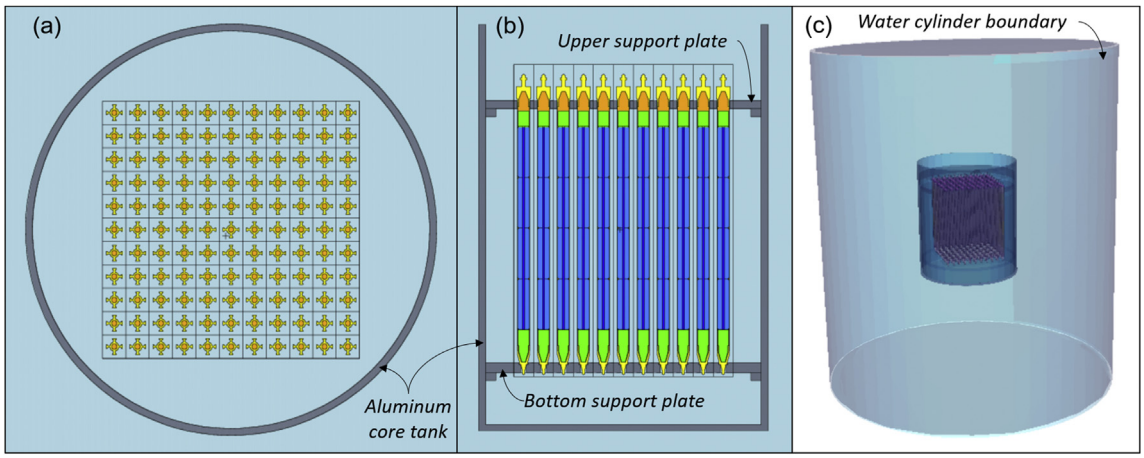

Fig. 3. (a) x-y plane and (b) x-z plane cross-section views of the MCNP model for the 11 × 11 square lattice at 5 cm pitch. (c) 3D view of the core assembly in a water cylinder boundary.

delayed neutron fraction β_{eff} of the SRA is also determined using two different calculation methods. The first calculation is based on the method developed in Ref. [24]:

$$\beta_{eff} = 1 - \frac{k_{eff,p}}{k_{eff}} , \tag{4}$$

where, $k_{eff,p}$ is the prompt neutron multiplication factor obtained from simulating the system without accounting for the delayed neutrons. The second calculation utilized the built-in KOPTS card, which calculates the adjoint weighted kinetic parameters β_{eff} and Λ in a single run [24–26].

KCODE calculations were executed with 2100 active cycles, 100 inactive cycles and 5×10^5 neutrons per cycle, which corresponds to 10^8 neutron histories. This is performed for all 36 fuel configurations to obtain k_{eff} vs pitch plots for each of the 6 square lattices as well as for the final configuration to obtain β_{eff}. The plots obtained from these criticality calculations is used as the basis for identifying the fuel configuration which closely meets the requirements for the SRA.

3.3. Reactor physics and kinetics calculations

To further characterize the selected SRA configuration, a hypothetical NS, with geometry dimensions that closely follow that of the TRIGA fuel rod, was incorporated in the model. A cylindrical NS with a diameter of 2.9 cm and length of 3.81 cm is declared at the center (0, 0, 33.905) of the SRA. Due to its long half-life and low gamma intensity, a ^{239}PuBe neutron source with spectrum (Fig. 4) obtained from Ref. [27] was employed. Exact composition of the ^{239}PuBe neutron source depends largely on the manufacturer. As such, the material composition of our hypothetical NS followed the values reported in Ref. [28], i.e. 68.6 wt % ^{239}Pu and 30.7 wt % ^{9}Be.

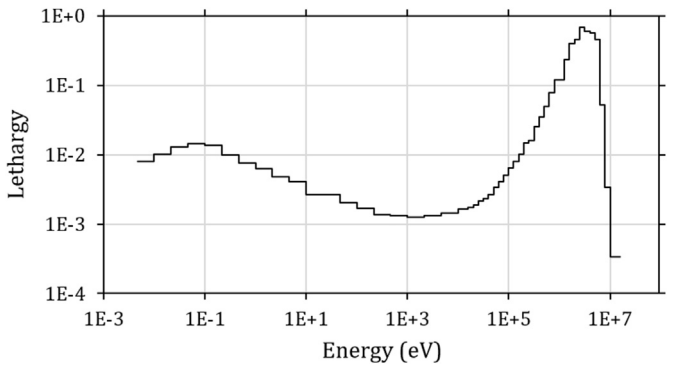

Fig. 4. Bare ^{239}PuBe neutron spectra obtained from Ref. [27].

The mean neutron generation time Λ of the system was likewise calculated following the method presented in Ref. [29]:

$$\Lambda = \frac{\rho - \beta_{eff}}{\alpha_0} , \tag{5}$$

where $\rho = \frac{k_{eff}-1}{k_{eff}}$ is the reactivity of the system. The fundamental mode decay constant, α_0 is obtained by simulating the prompt neutron decay in the SRA. This is done by implementing a fixed source calculation with the NS turned on for 10 ms and then turned off. The neutron flux over all the fuel rods is then tallied as a function of time to calculate the prompt drop. The mean neutron generation time determined from this method is then compared with the value calculated with the KOPTS card as described in Section 3.2.

One of the proposed utilization for the SRA is neutron irradiation to induce small amounts of radioactivity in selected materials. In order to effectively implement this application, it is essential to determine the neutron distribution in the SRA. For this purpose, the neutron flux distribution in the SRA is calculated in 0.125 cm^3 meshes through the whole space of interest. The lethargy neutron spectra and relative distribution of thermal, epithermal, fast and total neutrons were likewise determined in selected regions of the system.

4. Results and discussion

4.1. k_{eff} vs Pitch plots

Calculated k_{eff} corresponding to different fuel pitches are plotted in Fig. 5 (a) for each of the six fully filled fuel arrays. The uncertainties of all calculated effective multiplication factors ranged from 7 pcm to 9 pcm. Maximum k_{eff} values are observed at about 4 cm pitch for all the square lattices considered. The plots show that 8 × 8 to 11 × 11 configurations result in supercritical assemblies when the fuel pitch is less than 5 cm. On the other hand, the maximum k_{eff} calculated for the 6 × 6 configuration is 0.92557

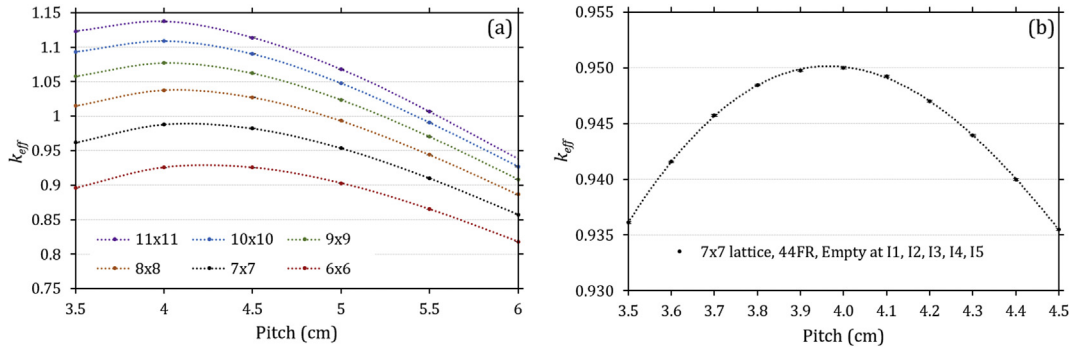

Fig. 5. k_{eff} versus fuel pitch for (a) different square lattices filled with TRIGA fuel rods and (b) 7 × 7 fuel rod lattice with 5 empty slots at I1, I2, I3, I4 and I5.

± 0.00008 at 4 cm. This value is 2.64% $\Delta k/k$ lower than our target, which indicate that the best candidate for the SRA is the 7 × 7 square lattice. These results provide information on the criticality state of the system with different number of fuel rods and can help establish the safety margins for the SRA.

Since the SRA core is intended to contain the NS and other instrumentation, different configurations of empty slots in the 7 × 7 square lattice were investigated until the k_{eff} vs fuel pitch plot in Fig. 5 (b) was obtained. This plot is derived from a 7 × 7 square lattice with 44 TRIGA fuel rods and 5 empty slots, which results in a subcritical configuration with a maximum k_{eff} value of 0.95001±9 *pcm* at 4 cm pitch. The 5 empty slots are labeled from I1 to I5 as shown in Fig. 6. The NS will be positioned at I1 to preserve the symmetry of the system and to ensure maximum external source efficiency, while positions I2 to I5 are proposed to be used as inner irradiation channels. 64 smaller circular holes (⌀ = 1.5 cm) and 8 bigger holes (⌀ = 5 cm) were also added at the support plates to provide slots for neutron detectors and outer irradiation channels, respectively. The labeling scheme applied and the schematic diagram of the selected SRA configuration are presented in Figs. 6 and 7, respectively.

4.2. SRA neutron flux profile

A hypothetical neutron source (NS) is added in the selected SRA configuration as described in Section 3.3. The system is then characterized by mapping the neutron flux distribution at 3 horizontal planes. The first map in Fig. 8 (a) is obtained at z = 34.5 cm, which cuts across the volumetric neutron source as indicated by the red line in Fig. 7. It is observed that in this plane, the neutron distribution of the NS dominates as predicted by Eq. (3). At planes farther from the source, z = 49.25 cm and z = 64.25 cm, the neutron distribution becomes more uniform and tends to take the form of the fuel rods arrangement in the lattice. This indicates that at locations farther from the NS, neutrons born from fission become increasingly important in comparison to the neutrons from the NS. These neutron profile patterns resemble what has been previously reported for subcritical assemblies [1], [2]. It is also noted that at z = 64.25 cm, which is just above the top graphite reflectors of the fuel rods, the neutron flux is highest at the central part of each lattice slot due to the absence of fuel materials in this plane.

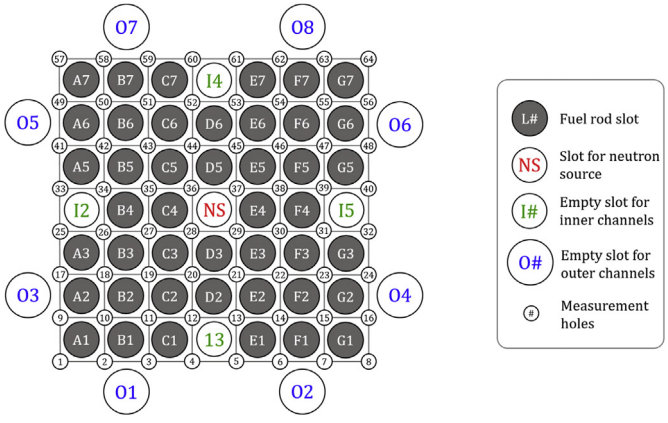

Fig. 6. Core configuration with labeling scheme used to identify slots in the SRA.

Neutron spectra in six representative channels (I2, O1, MH1, MH10, MH19, MH28) in the SRA are characterized. Due to symmetry of the SRA configuration, the inner channel I2 is expected to have the same flux distribution as I3, I4 and I5. For outer channels, O1 has the same flux distribution as O2 to O8. Measurement holes (MH) 1, 10, 19 and 28 are also considered to provide information on the neutron flux distribution in channels situated at 4 different radial distances from the NS.

Fig. 9 shows a comparison of the neutron spectra in the six representative channels of the SRA, where the flux values are normalized to the corresponding value at 1 eV. The spectral fractions for thermal, epithermal and fast neutrons are summarized in Table 1, which also shows the relative magnitude of the total flux, φ_{tot} in each channel. The highest total flux is obtained at MH28, which is located closest to the NS. This channel also registers the hardest spectrum with ~40% fast neutrons. The high thermal spectral fraction (~70%) in O1 makes it ideal for thermal neutron activation applications, although it may require considerably long irradiation time due to the low total flux in this channel that is only 25% of the total flux in MH28. The second best candidate for thermal neutron irradiation applications is I2 with 36% more neutrons than O1 and 53.1% neutrons in the thermal energy range.

4.3. SRA kinetic parameters

The total (k_{eff}) and prompt ($k_{eff,p}$) neutron multiplication factors of the SRA with the hypothetical NS were found to be 0.95286±3 pcm and 0.94574±3 pcm, respectively. These factors are used together with Eq. (4) to calculate the delayed neutron fraction of the system, which was evaluated to be β_{eff} = 747.2 pcm±4.5 pcm. Although the hypothetical NS increased the k_{eff} of the system by 0.3% $\Delta k/k$ from 0.95001, the factor is still within the range considered for the SRA.

The simulation of the prompt neutron decay described in Section 3.3 resulted in the plot shown in Fig. 10. An exponential function is fitted, using the method of least squares, in the prompt drop region and the decay constant was evaluated to be α_0 = 1.318.

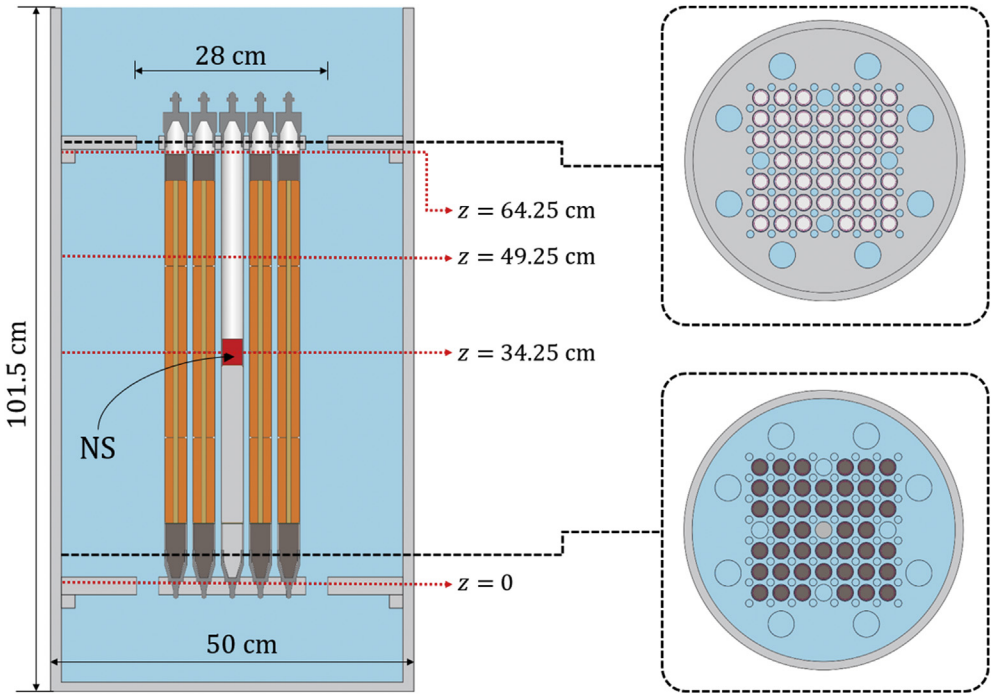

Fig. 7. Schematic diagram for the selected subcritical configuration with 44 TRIGA fuel rods, 5 empty slots and measurement holes arranged in a 7 × 7 square lattice.

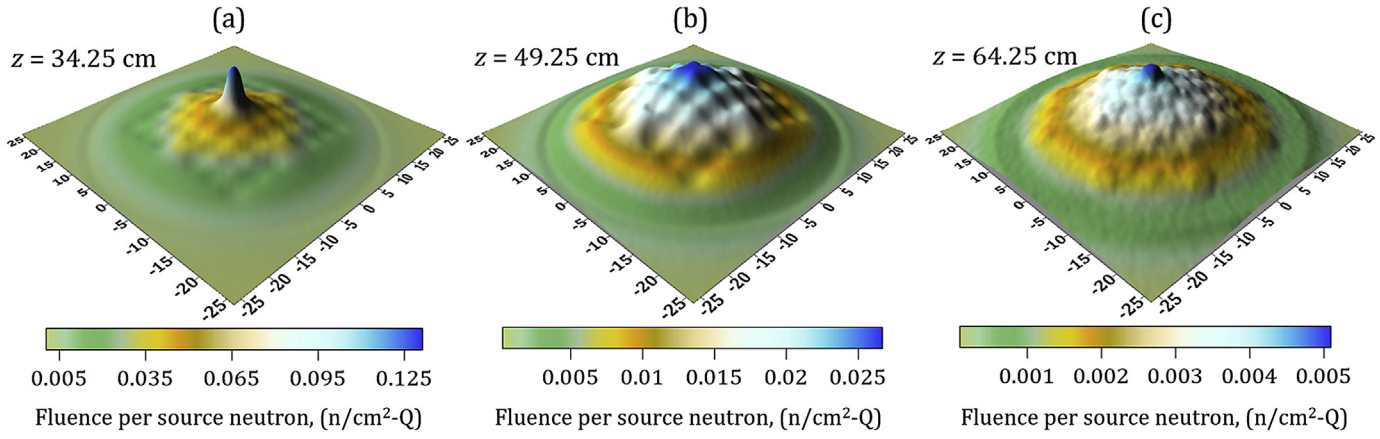

Fig. 8. Spatial neutron distribution in the SRA at (a) $z =$ 34.25 cm, (b) $z =$ 49.25 cm, and (c) $z =$ 64.25 cm. Tallies are calculated in 0.125 cm^3 meshes at 0.5 cm divisions in the x, y and z directions.

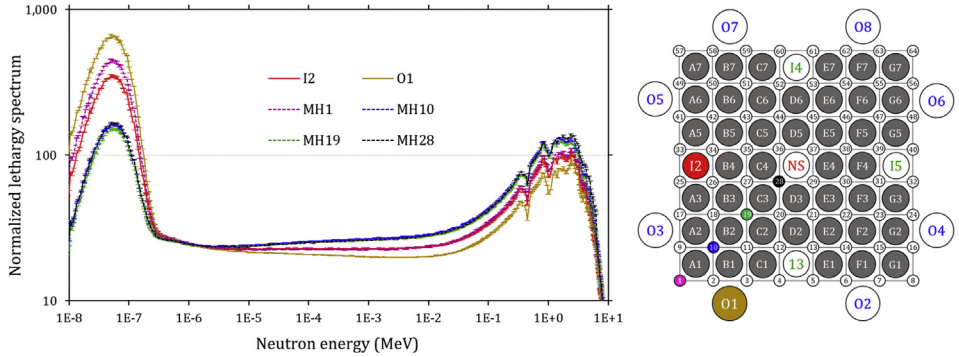

Fig. 9. Lethargy neutron spectrum at proposed irradiation channels I2 and O1 as well as measurement holes 1, 10, 19 and 28 in the SRA. Data is normalized to the corresponding value at 1 eV.

Table 1
Fractions of thermal (<625 eV), epithermal (0.625 eV–0.1 MeV), and fast (>0.1 MeV) neutron fluxes and relative magnitude of total neutron flux (φ_{tot}) in representative SRA channels.

Channel	Thermal (%)	Epithermal (%)	Fast (%)	Relativeφ_{tot} *
I2	53.1	22.0	24.8	0.61
O1	70.1	14.4	15.5	0.25
MH1	57.9	19.1	23.0	0.23
MH10	31.8	29.8	38.4	0.43
MH19	31.1	30.5	38.4	0.78
MH28	31.7	28.7	39.6	1.00

*Relative φ_{tot} is obtained by normalizing the total flux in each channel relative to the value in MH28.

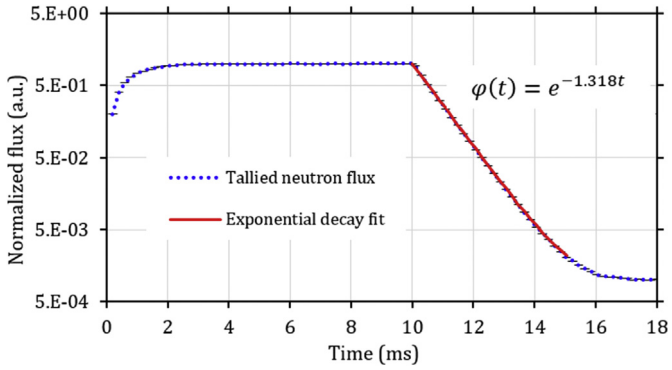

Fig. 10. Relative neutron flux averaged over all fuel elements as a function of time.

Table 2
Comparison of SRA kinetic parameters calculated using two different methods.

Parameter	Prompt method	Adjoint weighted
β_{eff}	747.2 pcm±4.5 pcm	748 pcm±7 pcm
Λ	~ 37 μs	41 μs

Using Eq. (5), the mean neutron generation time of the system is calculated to be $\Lambda = \sim 37$ μs. Table 2 compares the values of kinetic parameters obtained using the prompt method and the values calculated using the KOPTS card option in MCNP5. Results agree well for the calculated β_{eff} values. The discrepancy between the two calculated Λ values is due to the intrinsic difference of the calculation methods we applied. However, the ~10% difference in our calculations is small compared to reported values in Refs. [30] [31], where the difference between calculated values of the mean generation time can reach 36% for a bare system, more than 200% for a thermal fission system, and can even reach more than 600% for a fast fission system. It is also shown in Ref. [32] that different calculations methods can readily result in 10% difference in calculated values of reactor kinetic parameters. In addition, it must be noted that the values we calculated for the kinetic parameters of the SRA are well within the range of values summarized in Ref. [29].

5. Summary

The design for a subcritical reactor assembly (SRA) with 44 TRIGA fuel rods arranged in a 7 × 7 square lattice is proposed. The basic reactor physics parameters of the designed SRA are computed through the use of the neutron transport calculation code MCNP. It is found that the subcritical configuration results in a maximum k_{eff} value of 0.95001 ± 0.00009 at 4 cm pitch. The addition of a hypothetical neutron source increases the k_{eff} of the system by 0.3% $\Delta k/k$. The neutron distribution and spectra of the chosen core configuration is calculated to provide information that will be useful for the proposed utilization of the SRA for sample irradiation and reactor physics experiments. Lastly, the delayed neutron fraction and mean neutron generation time, which are key kinetic parameters of the system, were calculated using two different methods and were found to be 748 pcm±7 pcm and 41 μs, respectively. The result of this work will be the basis of the subcritical assembly that will be established at the PRR-1 facility in PNRI. The implementation of this facility is projected to reestablish nuclear science and technology expertise in the Philippines as well as demonstrate the reuse of a nuclear research reactor that has been unutilized for three decades.

Acknowledgements

This work was performed during A. Astronomo's fellowship training at Jožef Stefan Institute in Slovenia with the support of the IAEA TC PHI0015: Building Capacity in Nuclear Science and Technology by Re-establishing the PRR-1 as a TRIGA Fuel Subcritical Assembly. The efforts of the late Dr. Pablo Saligan to initiate the reoperation of PRR-1 is gratefully acknowledged. Special thanks to L. Leopando for developing a detailed SCALE model for the PRR-1 TRIGA fuel rod and to R. Gatchalian for converting the model into MCNP geometry. A. Astronomo is also grateful for valuable comments from K. Romallosa, F. Hila and J. Jecong.

Appendix A. Supplementary data

Supplementary data to this article can be found online at https://doi.org/10.1016/j.net.2018.09.025.

References

[1] H.R. Vega-Carrillo, I.R. Esparza-Garcia, A. Sanchez, Features of a subcritical nuclear reactor, Ann. Nucl. Energy 75 (2015) 101–106.
[2] N. Xoubi, Calculation of the power and absolute flux of a source driven subcritical assembly using Monte Carlo MCNP code, Ann. Nucl. Energy 97 (2016) 96–101.
[3] G. Klujber, J.L. Kloosterman, D. De Haas, Neutron noise measurements at the delphi subcritical assembly, in: Proc. PHYSOR 2012 Adv. React. Phys. - Link. Res. Ind. Educ, 2012, pp. 1–18.
[4] A. Talamo, et al., MCNPX, MONK, and ERANOS analyses of the YALINA Booster subcritical assembly, Nucl. Eng. Des. 241 (5) (2011) 1606–1615.
[5] N. Xoubi, Neutronic design study of accelerator driven system (ADS) for Jordan subcritical reactor as a neutron source for nuclear research, Appl. Radiat. Isot. 131 (2018) 71–76.
[6] C.D. Bowman, et al., Nuclear energy generation and waste transmutation using an accelerator-driven intense thermal neutron source, Nucl. Instrum. Methods Phys. Res. A 320 (1–2) (1992) 336–367.
[7] C. Rubbia, et al., Conceptual Design of a Fast Neutron Operated High Power Energy Amplifier, 1995. CERN/AT/95-44.
[8] G. Perret, et al., Kinetic parameter measurements in the MINERVE reactor, IEEE Trans. Nucl. Sci. 64 (1) (2017) 724–734.
[9] A. Herrera-Martínez, Y. Kadi, G. Parks, M. Dahlfors, Transmutation of nuclear waste in accelerator-driven systems: fast spectrum, Ann. Nucl. Energy 34 (7) (2007) 564–578.
[10] Z. Chen, Y. Wu, B. Yuan, D. Pan, Nuclear waste transmutation performance assessment of an accelerator driven subcritical reactor for waste transmutation (ADS-NWT), Ann. Nucl. Energy 75 (2015) 723–727.
[11] W. Kim, H.C. Lee, C.H. Pyeon, H.C. Shin, D. Lee, Monte Carlo analysis of the accelerator-driven system at kyoto university research reactor Institute, Nucl. Eng. Technol. 48 (2) (2016) 304–317.
[12] C. Rubbia, et al., Neutronic Analyses of the Trade Demonstration Facility, vol. 5639, 2004, pp. 103–123. October.
[13] X-5 Monte Carlo Team, "MCNP - a General Monte Carlo N-particle Transport Code, Version 5." LA-CP-03-0245, LANL, 2003.
[14] A. Dall'Osso, The influence of the neutron source spectrum on the infinite homogeneous reactor in subcritical condition, Ann. Nucl. Energy 77 (2015) 408–414.
[15] Z.I. Zafar, M.H. Kim, Embedded fission source approach to analyze external source effect in a subcritical reactor, Nucl. Eng. Des. 327 (2018) 238–247. April 2016.
[16] N. Xoubi, Neutrons and gamma-ray dose calculations in subcritical reactor

facility using MCNP, Atoms 4 (3) (2016) 20.
[17] A. Gandini, On the multiplication factor and reactivity definitions for subcritical reactor systems, Ann. Nucl. Energy 29 (6) (Apr. 2002) 645–657.
[18] K. Nishihara, T. Iwasaki, Y. Udagawa, A new static and dynamic one-point equation and analytic and numerical calculations for a subcritical system, J. Nucl. Sci. Technol. 40 (7) (2003) 481–492.
[19] H. Shahbunder, C.H. Pyeon, T. Misawa, J.Y. Lim, S. Shiroya, Subcritical multiplication factor and source efficiency in accelerator-driven system, Ann. Nucl. Energy 37 (9) (2010) 1214–1222.
[20] S. Zhou, et al., LAVENDER: a steady-state core analysis code for design studies of accelerator driven subcritical reactors, Nucl. Eng. Des. 278 (2014) 434–444.
[21] M. Türkmen, Ü. Çolak, Ş. Ergün, Effect of burnup on the neutronic parameters of ITU TRIGA Mark II research reactor, Prog. Nucl. Energy 83 (2015) 26–34.
[22] Ž. Štancar, L. Barbot, C. Destouches, D. Fourmentel, J.F. Villard, L. Snoj, Computational validation of the fission rate distribution experimental benchmark at the JSI TRIGA Mark II research reactor using the Monte Carlo method, Ann. Nucl. Energy 112 (2018) 94–108.
[23] M.B. Chadwick, et al., ENDF/B-VII.0: next generation evaluated nuclear data library for nuclear science and technology, Nucl. Data Sheets 107 (12) (2006) 2931–3060.
[24] R.K. Meulekamp, S.C. Van Der Marck, Calculating the effective delayed neutron fraction with Monte Carlo, Nucl. Sci. Eng. 152 (August) (2006) 142–148.
[25] B.C. Kiedrowski, et al., "MCNP5-1.60 Feature Enhancements & Manual Clarifications," No. LA-UR-10-06217, 2010.
[26] R. Henry, I. Tiselj, L. Snoj, Analysis of JSI TRIGA MARK II reactor physical parameters calculated with TRIPOLI and MCNP, Appl. Radiat. Isot. 97 (2015) 140–148.
[27] International Atomic Energy Agency (IAEA) TRS 403, Compendium of Neutron Spectra and Detector Responses, 2001, p. 276, 403.
[28] N. Xu, et al., Elemental composition in sealed plutonium-beryllium neutron sources, Appl. Radiat. Isot. 95 (2015) 85–89.
[29] L. Snoj, A. Kavčič, G. Žerovnik, M. Ravnik, Calculation of kinetic parameters for mixed TRIGA cores with Monte Carlo, Ann. Nucl. Energy 37 (2) (2010) 223–229.
[30] B. Verboomen, W. Haeck, P. Baeten, Monte Carlo calculation of the effective neutron generation time, Ann. Nucl. Energy 33 (10) (2006) 911–916.
[31] M. Hassanzadeh, S.A.H. Feghhi, H. Khalafi, Calculation of the neutron importance and weighted neutron generation time using MCNIC method in accelerator driven subcritical reactors, Nucl. Eng. Des. 262 (2013) 404–408.
[32] R.K. Meulekamp, S.C. Van Der Marck, Calculating the effective delayed neutron fraction with Monte Carlo, Nucl. Sci. Eng. 152 (2006) 142–148.